

Supporting Information

Experimental section

Synthesis of spinnable carbon nanotube array. Spinnable carbon nanotube (CNT) arrays were synthesized by chemical vapor deposition with Fe/Al₂O₃ on a silicon substrate as the catalyst at 740 °C. To produce Fe/Al₂O₃ catalyst, electron beam evaporation was applied to deposit Fe (1.2 nm) and Al₂O₃ (3 nm) on silicon substrate at rates of 0.5 and 2 Å/s, respectively. C₂H₄ was chosen as the carbon source, while Ar and H₂ were chosen as the carrier gas. The flow rates of H₂, C₂H₄ and Ar were 30, 90 and 400 sccm, respectively.

Blood flow measurement. Five healthy adult volunteers (ages from 20 to 30 years old) were included in the measurement and they were consented to all the relative tests. During the test, the arm was fixed under sitting position and then a fixed area of 5.1 × 3.7 cm² at the forearm was scanned through a laser Doppler perfusion imager. The blood flow tests of all the volunteers were first measured after resting for 20 min. After heating treatment with a thermochromic resistive heater (TRH) textile at ~ 40 °C for 10 min, the blood flow was measured again. Finally, the mean value of blood flow flux was calculated by the built-in software.

Characterization. The morphology of TRH was characterized by scanning electron microscope (S-4800, Hitachi) operated at 1 KV. The microstructure of CNTs was observed by transmission electron microscopy (JEM-2100 F, JEOL). All the thermal properties and images were obtained from an infrared camera (PI 450, Optris). Average temperatures of the devices were measured throughout the work. Photographs were taken by a camera (J1, Nikon). Stretching test was realized by a table-top universal testing instrument (HY-0350, Hengyi). DC bias voltage was supplied by a programmable DC source meter (M8813, Maynuo). The blood flow was tested by a laser Doppler perfusion imager (LDI2-HIR, Moor).

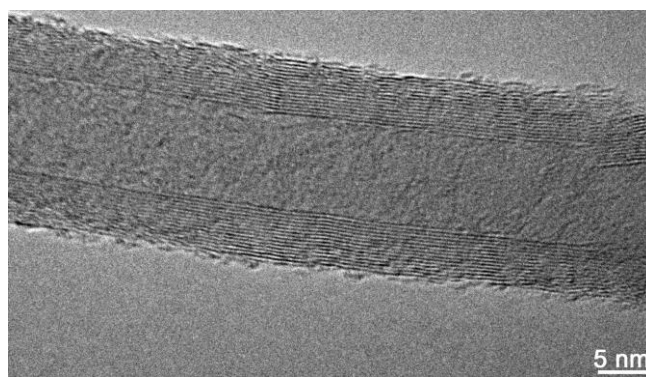


Fig. S1 High resolution transmission electron microscope image of the CNT.

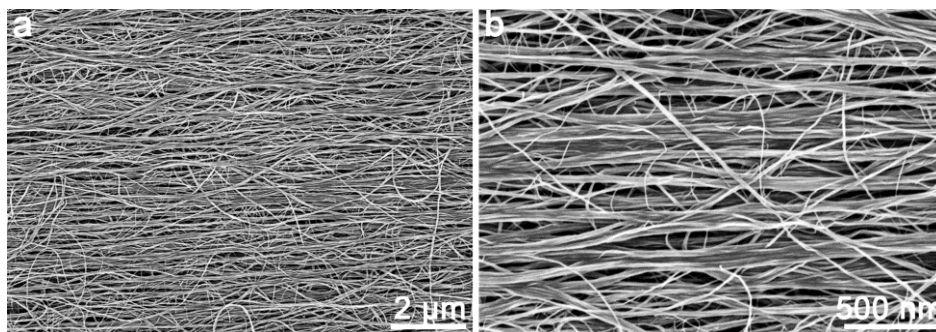


Fig. S2 Scanning electron microscope images of 1.8- μm -thick CNT sheet paved on the copper foil at low (a) and high (b) magnifications.

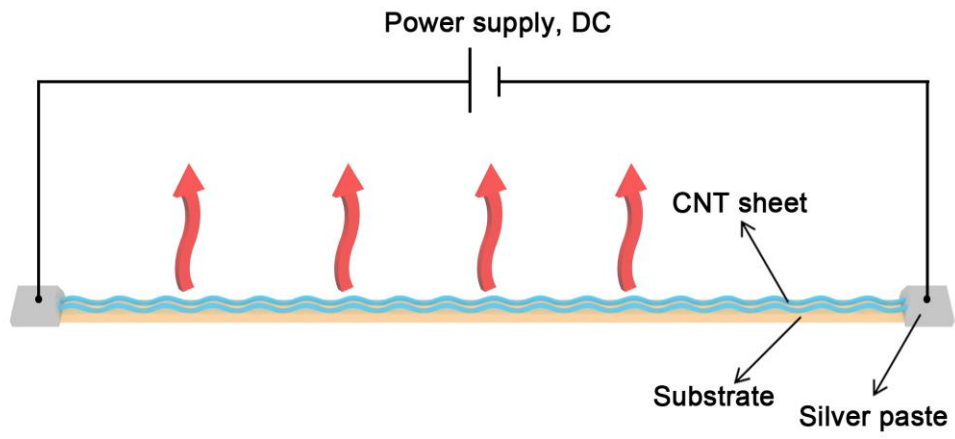


Fig. S3 Schematic illustration to show the working mechanism of the strip-shaped TRH.

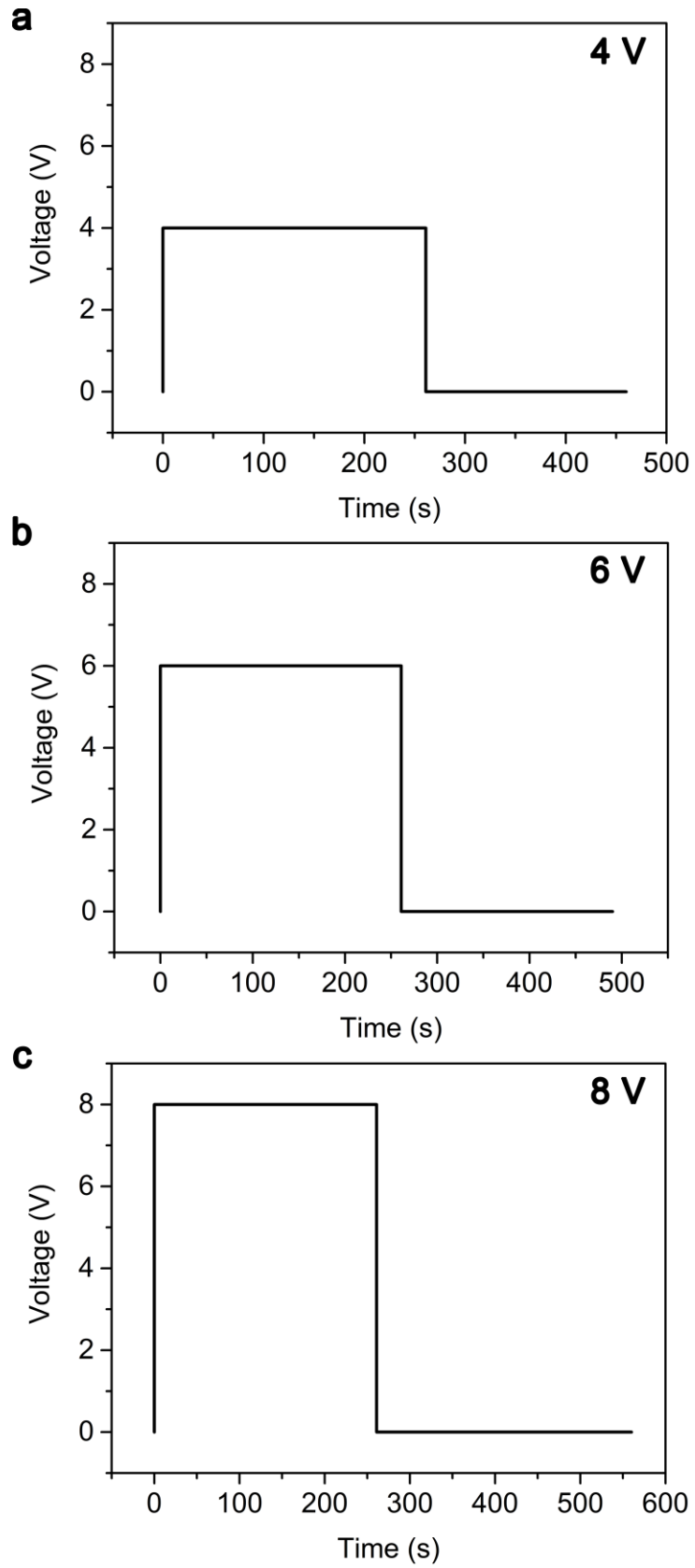


Fig. S4 Voltage-time curves applied on the strip-shaped TRH.

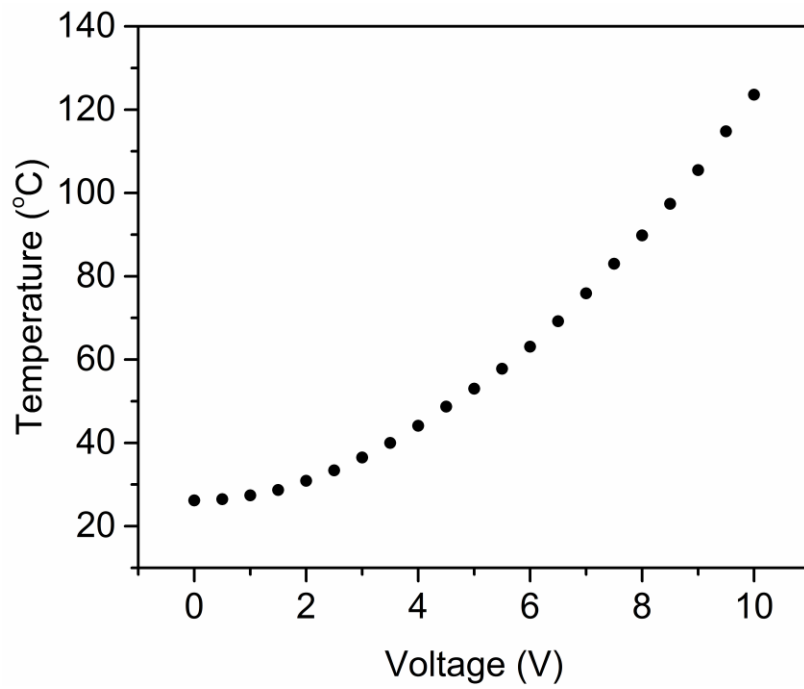


Fig. S5 Dependence of saturated temperature on voltage.

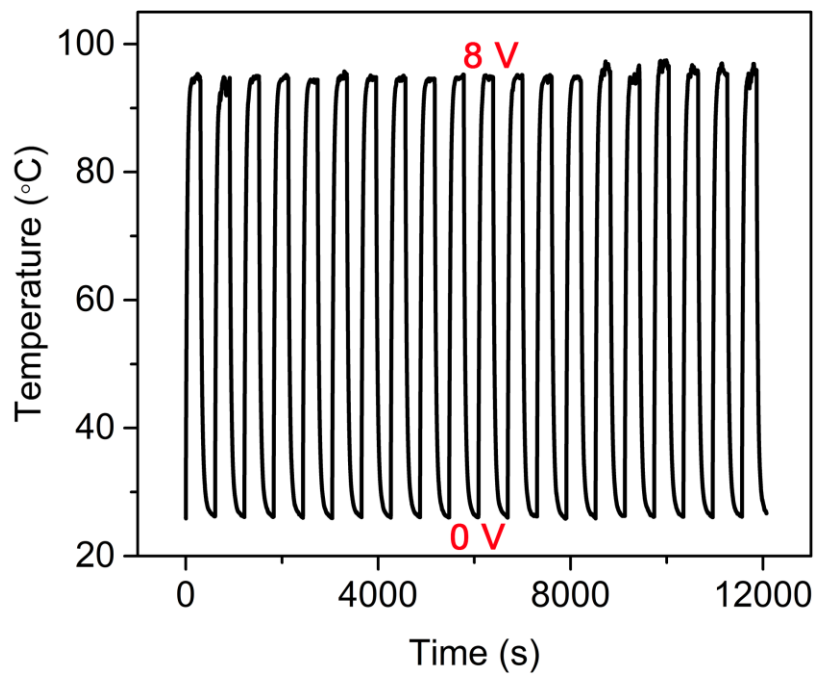


Fig. S6 Temperature-time curve of the strip-shaped TRH under pulsed voltages between 0 and 8 V.

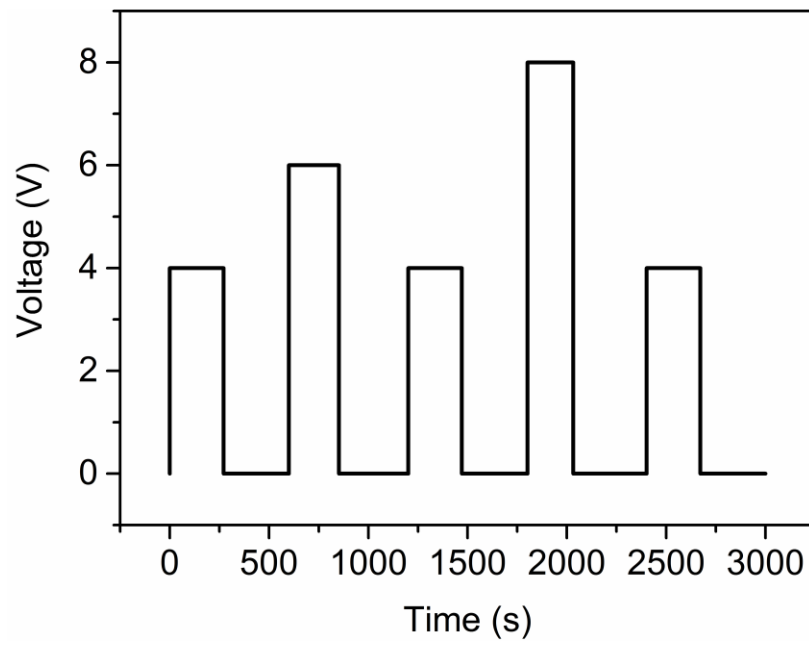


Fig. S7 Voltage-time curve applied on the strip-shaped TRH.

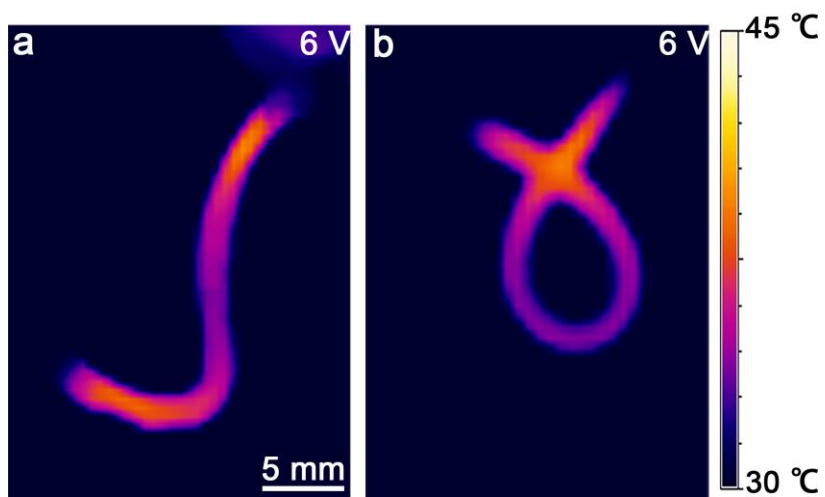


Fig. S8 Infrared images of a strip-shaped TRH after deformation into different shapes.

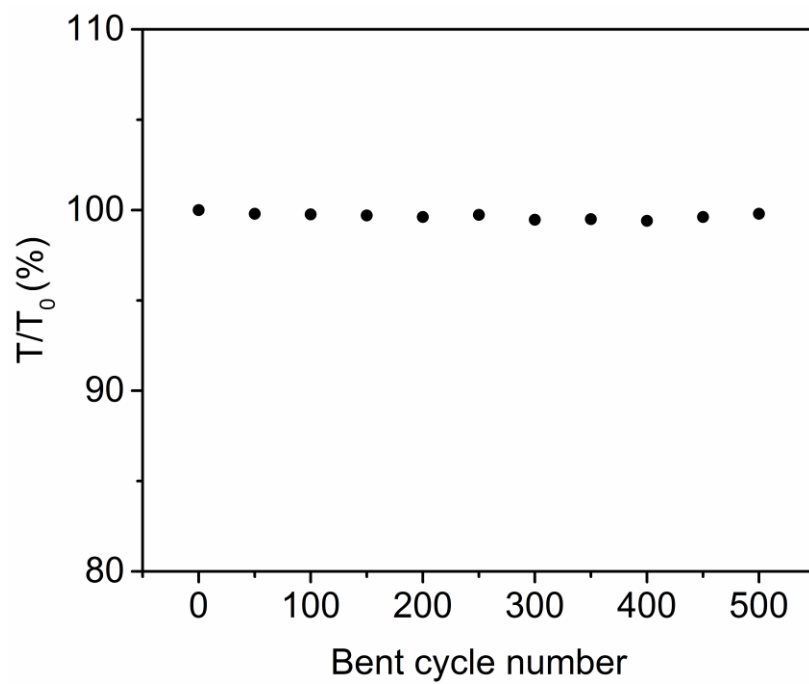


Fig. S9 Dependence of saturated temperature on bent cycle. Here T_0 and T correspond to the saturated temperatures before and after bending, respectively.

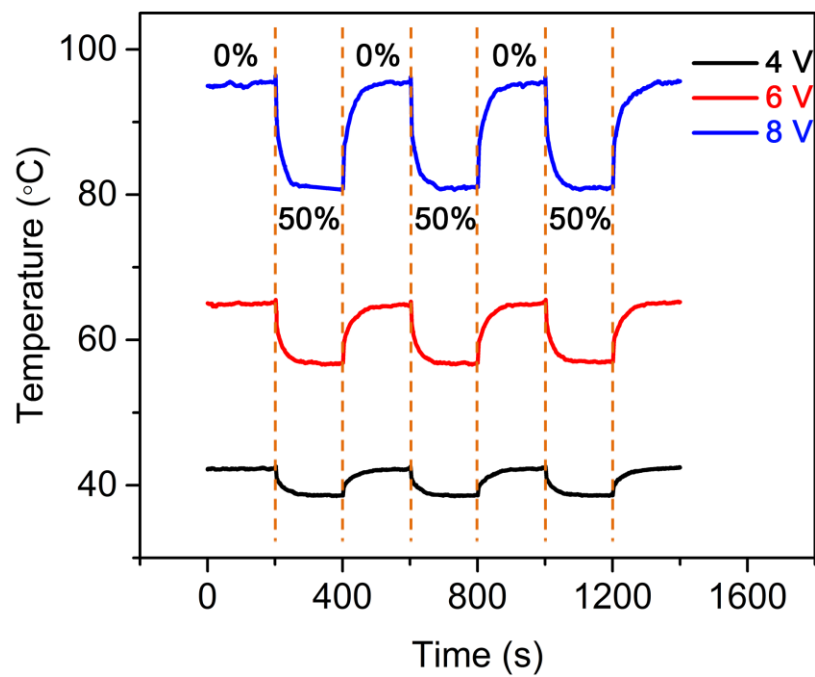


Fig. S10 Temperature-time curve of the strip-shaped TRH during repeatable stretching to 50% and releasing.

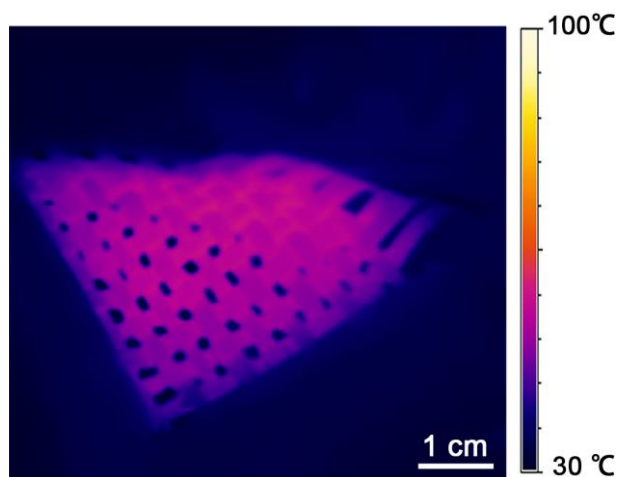


Fig. S11 Infrared image of a TRH textile under three-dimensional distortion at 6 V.

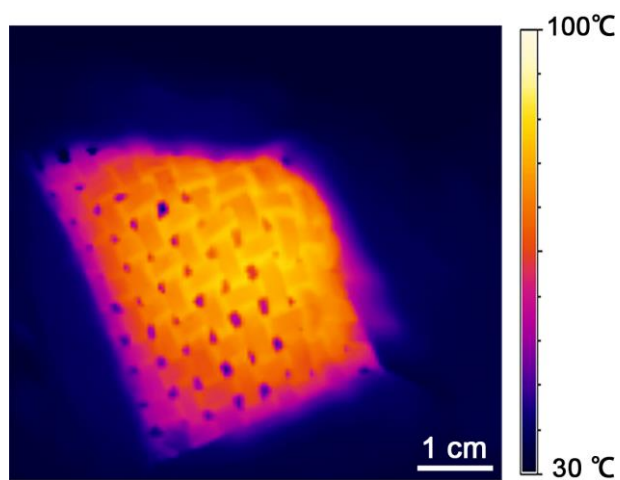


Fig. S12 Infrared image of a TRH textile under three-dimensional distortion at 7.5 V.

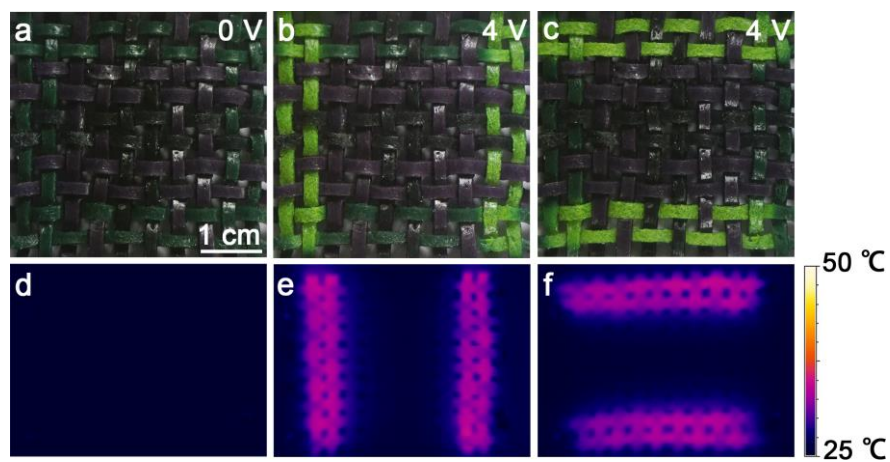


Fig. S13 (a-c) Photographs of the TRH textile being selectively applied with voltages. (d-f) The corresponding temperature distributions of the textile at (a-c).

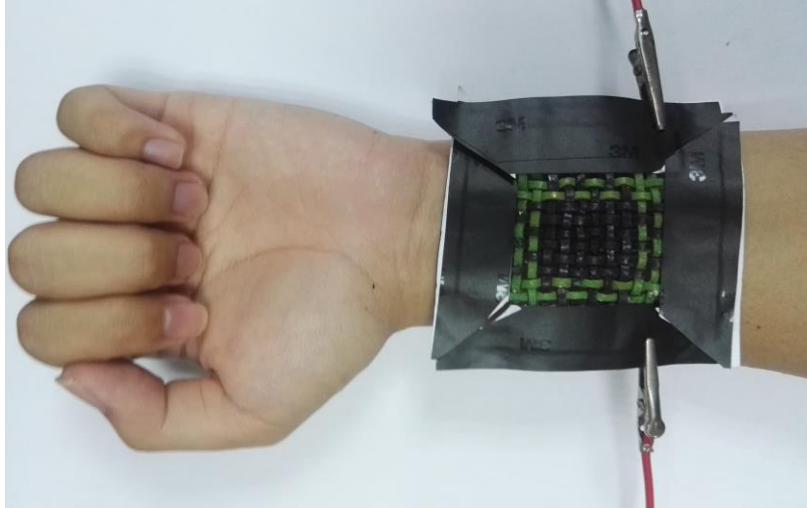


Fig. S14 Photograph showing the heating process with the TRH textile.